Protein Science (1996), 5:414-421. Cambridge University Press. Printed in the USA.

A novel, multilayer structure of a helical peptide

K.S. TAYLOR,[1] M.-Z. LOU,[1] T.-M. CHIN,[2] N.C. YANG,[2] AND R.M. GARAVITO[1]

[1] Department of Biochemistry and Molecular Biology, The University of Chicago, Chicago, Illinois 60637
[2] Department of Chemistry, The University of Chicago, Chicago, Illinois 60637

(RECEIVED October 2, 1995; ACCEPTED December 27, 1995)

Abstract

X-ray diffraction analysis at 1.5 Å resolution has confirmed the helical conformation of a de novo designed 18-residue peptide. However, the crystal structure reveals the formation of continuous molecular layers of parallel-packed amphiphilic helices as a result of much more extensive helix–helix interactions than predicted. The crystal packing arrangement, by virtue of distinct antiparallel packing interactions, segregates the polar and apolar surfaces of the helices into discrete and well-defined interfacial regions. An extensive "ridges-into-grooves" interdigitation characterizes the hydrophobic interface, whereas an extensive network of salt bridges and hydrogen bonds dominates the corresponding hydrophilic interface.

Keywords: amphiphilicity; de novo design; helix packing; peptide assembly; water-mediated contacts

How an amino acid sequence determines the three-dimensional structure of a protein remains a major subject of investigation, and one approach toward answering this question is through the study of peptide assemblies that mimic the behavior of globular proteins. Pioneering work by DeGrado and coworkers has yielded the design principles for the hexadecapeptides α1A and α1B, which self-associate to form stable, helical tetramers in aqueous solution (DeGrado et al., 1987, 1989; Ho & DeGrado, 1987; DeGrado, 1988), constituting de novo supramolecular systems. Other de novo systems have now been synthesized and characterized (Handel & DeGrado, 1990; Hecht et al., 1990; Regan & Clarke, 1990; O'Shea et al., 1991; Handel et al., 1993; Kamtekar et al., 1993; Choma et al., 1994; Harbury et al., 1994; Lutgring & Chmielewski, 1994; Robertson et al., 1994), and the crystal structures of a few amphiphilic peptide aggregates have been determined by X-ray analysis (Hill et al., 1990; O'Shea et al., 1991; Lovejoy et al., 1993; Schafmeister et al., 1993; Harbury et al., 1994; Prive et al., 1995). Because the α-helix is a fundamental secondary structural feature in many naturally occurring proteins, the three-dimensional structures of these self-assembling systems have revealed subtle details of helix packing found in nature (Harbury et al., 1993).

Whereas the creation and modeling of de novo soluble proteins have received the most attention, the creation of peptide mimics of ion channel proteins from an amphiphilic helical motif has also been a focus of research (Lear et al., 1988; Montal, 1995). Although helical channel-forming peptides, such as alamethacin (Fox & Richards, 1982; Banerjee et al., 1983), often have very high apolar–polar amino acid ratios, more polar peptides like melittin (Terwilliger et al., 1982), peptide M2 (Oblatt-Montal et al., 1993), and the $(LSSLLSL)_3$ peptide (Lear et al., 1988) can form discrete ion channels. For many of these channel-forming peptides, the consensus is that discrete channels are created upon the assembly of helical monomers into a membrane-integrated oligomer (Lear et al., 1988; Oblatt-Montal et al., 1993; Montal, 1995). Interestingly, a new class of amphiphilic lytic peptides, called magainins, have been discovered (Cruciani et al., 1991, 1992). These peptides tend to have ratios of apolar-to-polar amino acids approaching unity and can still interact directly with a lipid bilayer (Juretic et al., 1994; Tytler et al., 1995), although questions remain as to the degree of magainin integration into a lipid bilayer (Bechinger et al., 1991; Cruciani et al., 1992; Matsuzaki et al., 1995).

How helical peptide structure, peptide amphiphilicity, and specific amino acid distribution influence the formation of unique soluble peptide bundles or ion channels is still not clear, particularly for "chimeric" proteins such as melittin, which have soluble and membrane-integrated forms. Yang and colleagues (Chin et al., 1992; Hu et al., 1993) have tried to address this question with the synthesis of two amphiphilic octadecapeptides, peptide F (EQLLKALEFLLKELLEKL) and peptide W (EQL LKALEWLLKELLEKL), which have higher apolar–polar amino acid ratios (10:8) than peptides α1A and α1B (both 6:10). To enhance the potential for interhelical interactions, the design of the α-helix had eight apolar amino acids in two neighboring rows of four (i.e., Leu 3–Leu 4, Ala 6–Leu 7, Leu 10–Leu 11, and Leu 14–Leu 15) on one surface. Such a feature was expected

Reprint requests to R. Michael Garavito at his present address: Department of Biochemistry, Biochemistry Building, Michigan State University, East Lansing, Michigan 48824-1319; e-mail: garavito@selene.bch.msu.edu.

to result in the formation of a closely knit helix bundle that would differ from the de novo designed four-helix bundles (Chin et al., 1992).

Peptides F and W possess a high degree of helicity and self-associate into hexamers in aqueous solution (Chin et al., 1992; Hu et al., 1993). Moreover, peptide F is soluble in apolar organic solvents or in aqueous solutions of the detergent SDS, and it maintains a helical conformation under these conditions (N.C. Yang, T.M. Chin, R.M. Garavito, in prep.). Recent proton NMR data strongly suggest that peptide F can also form organized and inverted helical assemblies in SDS detergent micelles (N.C. Yang et al., in prep.). The oligomerization of peptide F in different solvents therefore raises the question as to how more balanced amphiphilicity (i.e., a apolar–polar amino acid ratio near unity) may affect the ability of peptides to self-assemble in hydrophobic and hydrophilic environments. The structures of such peptides under different solvent conditions may provide insights into the selection of packing modes for amphiphilic helices, in solution or in the membrane. We report here the crystallization of peptide F in different solvent conditions and the X-ray crystal structure of one crystal form to 1.5 Å resolution.

Results

Crystal characterization and structure determination of the Type I crystal form

Two crystal forms of peptide F were identified as growing under distinctly different solvent conditions: Type I crystals grow in water/2-propanol solvent system at moderate ionic strength, whereas Type II crystals grow in 70% saturated ammonium sulfate with almost no organic solvent. The lattice parameters and space groups of the two forms were characterized (Table 1) and show no indication of a common packing mode. Native X-ray data on the Type I and II crystals were collected to 1.41 Å (Table 2) and 2.1 Å, respectively.

The unit cell parameters of the Type I crystals and a strong 5.4 Å peak in a native Patterson map along the *c*-axis suggested a distinctive pattern of close, parallel helix packing. Using an idealized octadeca(alanine) α-helix, the rotation and translation function analyses yielded a family of self-consistent solutions for the parallel packing of the helices in the unit cell; this result allowed the determination of the phases for the Type I crystal form with molecular replacement procedures in X-PLOR 3.1 (Brünger, 1992). For the high-salt Type II crystal form, preliminary results from rotation and translation function analyses reveal a family of related molecular replacement phase solutions that strongly suggest that peptide F packs as a parallel coiled-coil structure (K. Taylor & R.M. Garavito, unpubl. obs.).

A molecular replacement protocol, similar to that described by Schafmeister et al. (1993) was used to obtain initial phases for the Type I crystal diffraction data (see the Materials and methods). After iterative cycles of model building and structural refinement, all peptide atoms and nine water molecules were assigned in the final model, which had a crystallographic R = 17.0% and an R_{free} = 19.6% for all reflections between 8 and 1.5 Å. The final $2F_o - F_c$ electron density map showed the entire 18-residue peptide as a helix (Fig. 1); none of the electron density above 1.0σ was uninterpreted.

Table 1. *Peptide F crystal forms*

Crystal	a (Å)	b (Å)	c (Å)	α (°)	β (°)	γ (°)	sp grp
Type I	22.60	10.67	29.24	90	101.85	90	$P2_1$
Type II	36.7	36.7	49.4	90	90	90	$P4_22_12$

Table 2. *Type I crystal diffraction data*[a]

Parameter	Mo data	Cu data	Merged data
Observations (no.)	4,756	19,979	18,751
Unique obs >2σ [b]	1,467	2,293	2,360
Unique obs >4σ [b]	1,254	2,227	2,262
Overall completeness	88.3%	97.2%	99.5%
R_{merge}[c]	8.2	7.0	7.5

[a] Data to 1.7 Å were collected using an Enraf-Nonius FAST with Mo K_α radiation (at the small molecule X-ray facility, Department of Chemistry, University of Notre Dame) and merged with a 1.5-Å data set collected at University of Chicago on a FAST with Cu K_α radiation to yield a data set to 1.5 Å resolution.

[b] σ refers to the RMS deviation in intensity I.

[c] $R_{merge} = (\Sigma_i |I_i - \langle I_i \rangle|)/\Sigma_i |I_i|$, where $\langle I_i \rangle$ is an average of I_i over all symmetry-equivalent reflections.

Helix packing in the Type I crystal form

The crystal is formed by rows of close-packed, parallel helices (Fig. 2A and Kinemage 1) separated by the *b*-axis translation (10.67 Å); Leu 4, Ala 6, Leu 10, and Leu 15 form an interdigitating, hydrophobic contact surface between the parallel neighbors. The parallel packing of helices in the crystal is distinct from the parallel coiled-coil and has no features typical of coiled-coil structures (e.g., supercoil formation, "knobs-into-holes" packing, or the formation of ion pairs between side chains of parallel helices) (Crick, 1952; McLachlan & Stewart, 1975; O'Shea et al., 1991). The only polar interactions between the parallel helices observed (Fig. 2A and Kinemage 2) are: a salt bridge between Lys 17 and a neighboring carboxy terminus, and a hydrogen bond between Gln 2 and a neighboring amino terminus.

The amphiphilic nature of the helix surface results in one surface of a row of helices being hydrophobic and the other being hydrophilic (Fig. 2B). Although an individual row consists of parallel helices (oriented along the *b*-axis, as seen in Fig. 2A), the rows pack against each other such that each row is antiparallel to its two neighboring rows in the crystallographic *ab*-plane, as shown in Figure 2B. The crystallographic twofold screw axis therefore creates a planar superstructure of antiparallel helices where the interfaces between rows of helices alternate between hydrophobic (Fig. 3) and hydrophilic (Fig. 4). Finally, planes of antiparallel-packed helices stack (helix amino terminus to helix carboxy terminus) to create the macroscopic crystal (Fig. 5).

The helix axes are aligned within 14° of the *c*-axis, leading to a crossing angle of +28° between a pair of antiparallel helices (i.e., helices related by the crystallographic twofold screw axis). This crossing angle is commonly observed in four-helix bundle proteins (Weber & Salemme, 1980; Presnell & Cohen, 1989). The distance between adjacent antiparallel helices across the hy-

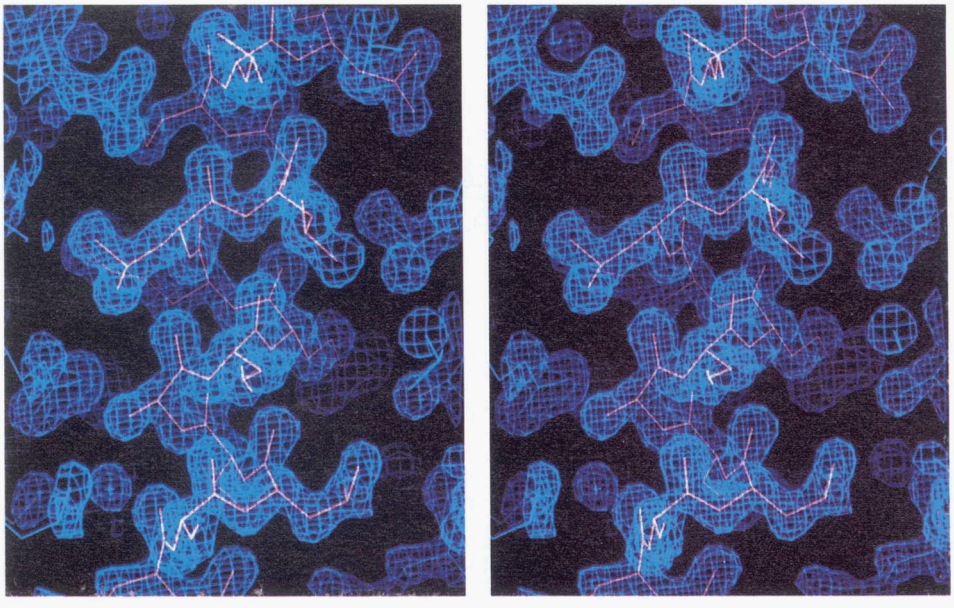

Fig. 1. Stereo view of representative $2F_o - F_c$ density viewed with the peptide helix axis vertical (residues 2–14 shown in red). Blue helix backbones represent symmetry-equivalent molecules and blue crosses represent symmetry-related water molecules. The electron density map is contoured at 1.3 σ.

drophobic interface is shorter than across the hydrophilic interface (10.3 Å versus 12.1 Å); i.e., the side chains from the antiparallel neighbors interdigitate much more so than do the hydrophilic side chains.

Helical deformations

Within each helix, 12 of the 14 main-chain intramolecular hydrogen bonds (in residues 1–16) are of the i, $i + 4$ type, representing typical α-helical behavior, and the phi-psi angles for these residues are in the most favored region for α-helical conformation (Kinemage 2). The average phi and psi angles for residues 2–15 are $-62 \pm 3°$ and $-42 \pm 4°$, respectively, agreeing quite well with that observed in globular proteins (Blundell et al., 1983; Chakrabarti et al., 1986). The final two hydrogen bonds in the helix, linking residues 16–18, are of the i, $i + 3$ type, corresponding to a 3_{10}-helical conformation (Ramachandran & Sasisekharan, 1968). The phi-psi angles for these residues show one with slightly distorted stereochemistry ($-87°$, $-4°$) and one in the typical 3_{10} configuration ($-63°$, $-16°$).

Although the cause of the transition from α- to 3_{10}-helix is not clear, the shift appears to improve the interactions between amino and carboxy termini of adjacent helices (Fig. 5). A sharp, dramatic bend in the helix, in the direction of the parallel helical neighbor $-b$ (see Fig. 2 for helix nomenclature), corresponds to the initiation of the 3_{10} region. This causes the C-terminus to point directly toward the N-terminus of the neighboring helix along the c-axis and results in a close interaction between these now adjacent helix termini. The α-to-3_{10}-helix transition also creates the interhelix salt bridge from Lys 17 to the carboxyl terminus of the neighboring helix $+b$ (Figs. 2A, 5). A second, more gradual type of helix curvature occurs over the entire helix length and in the direction of the a-axis across the apolar interface; this helix bending toward a hydrophobic packing surface has been described previously (Blundell et al., 1983).

The hydrophobic interface

The helix packing in the hydrophobic interface is characterized by both parallel and antiparallel elements (Kinemage 2). The class of antiparallel packing corresponds most closely to the 3–4 "ridges-into-grooves" convention (Chothia et al., 1981). However, in contrast to helix packing observed in antiparallel four-helix bundle proteins (Weber & Salemme, 1980; Presnell & Cohen, 1989), a semicircular ridge of leucines is formed by two parallel helices. The ridge then packs into the groove formed by three adjacent helices from the neighboring antiparallel row (Fig. 3), resulting in an interdigitation of ridges along the entire hydrophobic interface, analogous to the meshing of the teeth between two gears.

The ridge begins with Leu 3, Leu 7, and Leu 11 of helix b, representing an i, $i + 4$ spacing; the ridge then bends as it continues from Leu 11 to Leu 14 on helix b, representing an i, $i + 3$ spacing and then ends with Leu 18 from the adjacent helix $+b$ (Fig. 3). Leu 18 thus appears in a noncanonical position, aligning quite well on the ridge with Leu 11 and Leu 14 of the neighboring parallel helix. This atypical positioning arises from the 3_{10}-helix transition and helical bend at the C-terminus. A pair of parallel ridges separated by the b-axis translation thus creates the hydrophobic groove; the floor of the groove consists of the previously described residues involved in parallel helix contacts. In contrast to classical grooves formed by the i, $i + 3$ or i, $i + 4$ side-chain spacing on a single helix, this interhelical groove is wider, flatter, and more regular, allowing a close approach (10.3 Å) between the antiparallel rows of helices over the entire length of the helix. These features thus distinguish the helix packing described here from that typically observed in

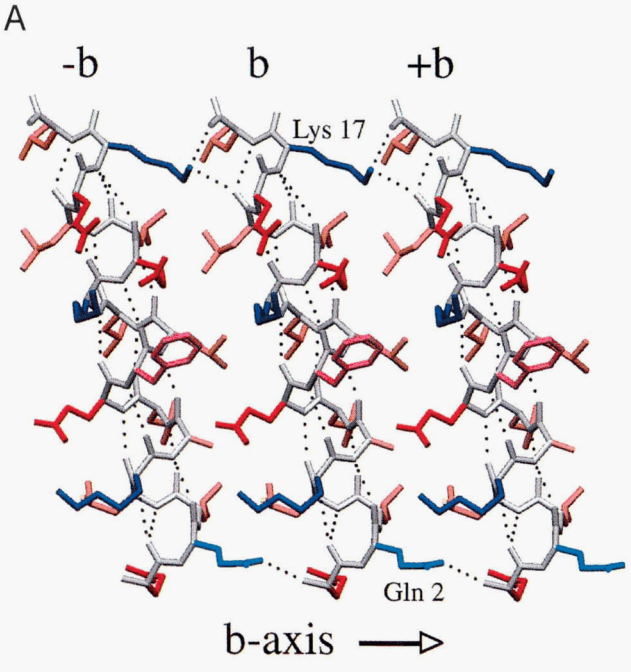

Fig. 2. Helix packing of peptide F in the Type I crystal form. **A:** View of parallel helices packed along the crystallographic *b*-axis; each helix, representing one unit cell translation, is labeled $-b$, b, and $+b$. Hydrogen bonding of main-chain atoms and two helix capping interactions (Gln 2 with the amino-terminal nitrogen and Lys 17 with a carboxy-terminal oxygen) are indicated. Brown, Leu and Ala side chains; blue, Lys; red, Glu; turquoise, Gln; magenta, Phe. **B:** Three rows of parallel helices related by the crystallographic 2_1 screw axis along *b* (horizontal) shows the helix packing in the *ab* crystal plane. Orientation of the figure is rotated 90° from the orientation in A, and looks roughly down the crystallographic *c*-axis (as well as the helix axes). Packing along the *a*-axis (vertical in the figure) demonstrates the alternating hydrophobic and hydrophilic nature of the helix interfaces (side chains colored according to A). Helices in each horizontal row are packed in an antiparallel manner with respect to the rows adjacent to it, thus the helices of row *a* run from carboxy terminus (nearest to viewer) to amino terminus and the helices of rows $-a$ and $+a$ run from amino terminus to carboxy terminus.

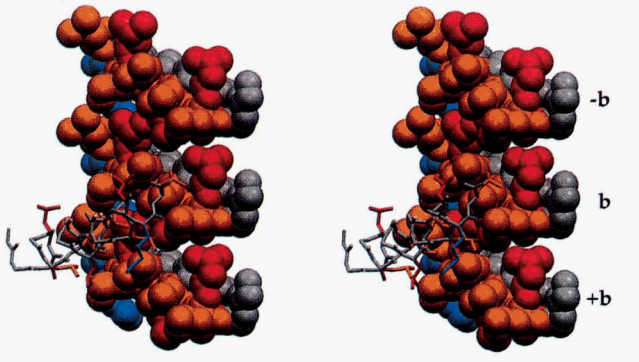

Fig. 3. Interactions between antiparallel helices across the hydrophobic interface. Van der Waals surfaces of three parallel helices ($-b$, b, and $+b$; helical axes roughly horizontal) reveal the grooves and ridges formed by protruding leucine residues (copper). Lys 17 (blue) is shown at the carboxy-terminal end of the helix. From right to left, Leu 4, Leu 7, Leu 11, and Leu 14 from helix *b* and Leu 18 from helix $+b$ make up one ridge; Leu 3, Ala 6, Leu 10, and Leu 15 (all in magenta) form the "floor" of the groove. An antiparallel helix (green backbone) demonstrates how the ridge of leucines packs into the groove: four of the leucines pack into one groove and Leu 18 packs into the neighboring groove.

globular proteins (Chothia et al., 1981). Whereas a typical globular α-helical protein forms a relatively spherical hydrophobic interior with varying helix–helix interactions, the hydrophobic interface in this supramolecular assembly is a regular and continuous two-dimensional "bilayer" of helices.

The polar interface

In the polar interface, each helix also interacts with two symmetry-related, antiparallel neighbors (e.g., helix *b* in Fig. 4 interacts with helices b' and $-b'$) via a complex network of

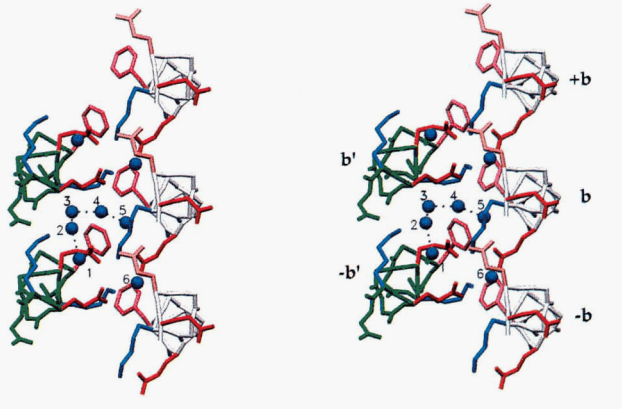

Fig. 4. Interactions between antiparallel helices across the hydrophilic interface. Three parallel helices ($-b$, b, and $+b$; white backbone) interact with two antiparallel neighbors ($-b'$ and b'; green backbone). Because the crystallographic 2_1 axis runs nearly perpendicular to the helix axes roughly at the level of Phe 9, a unique set of helix–helix interactions can be described using only half helices: only residues 1–9 for the white helices and residues 9–18 for the green helices are shown with all leucine and alanine side chains omitted. Hydrogen bonds between the water molecules (blue spheres) are indicated. The residue coloring scheme is the same as Figure 2A, except that Gln 2 is shown in copper.

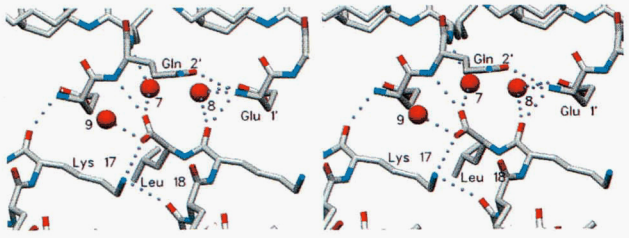

Fig. 5. Interactions at the interface between amino and carboxy termini. Capping interactions between termini involve contributions from four helices: $-b$ and b (lower half of the figure) and $-c'$ and c', corresponding to a c-axis unit translation (upper half of the figure). Lys 17 and Leu 18 are from helix $-b$ and helix b, respectively; Gln′ 2 arises from helix $-c'$, and Glu′ 1 is from neighboring parallel helix c'. Hydrogen bonds shown here involving water are listed in Table 3; not shown in this figure is the hydrogen bond between water 7 and $\epsilon 2$ oxygen of Glu 1 from a 2_1 symmetry-related neighbor. An elemental representation is used, where white represents carbon; red, oxygen; and blue, nitrogen. Waters 7, 8, 9 are shown as red spheres.

water-mediated hydrogen bonds and salt bridges. Of the nine water molecules assigned during refinement (Table 3), six are located at the hydrophilic interface between antiparallel helices. Five of these six water molecules make hydrogen bonds to each other in a head-to-tail fashion between one helix and its two antiparallel neighbors (Fig. 4). This chain of water molecules then forms a hydrogen bond network with side-chain atoms and main-chain atoms (Table 3), strengthening the interactions between each helix and its antiparallel neighbors. A large number of interactions between side chains of adjacent helices are not mediated by water. Hence, the wider separation of the polar interface, compared to the hydrophobic interface, probably favors the binding of water within the interface to occupy regions that would otherwise be vacant. These water molecules also add to the number of atoms packing between the helices within the wider, hydrophilic interface and serve to further increase the number of hydrogen bonding interactions between side chains.

Table 3. *Water-mediated hydrogen bonding interactions*[a]

Water molecule	H-bond partner		
	H_2O	Main-chain atom	Side-chain atom
W1	W2		
W2	W1, W3		
W3	W2, W4	Lys 12 O	
W4	W3, W5		Glu 16 Oϵ1
W5	W4	Lys 5 O	Glu 8 Oϵ1
W6		Gln 2 O	Lys5 Nζ
W7		Leu 3 N	Glu 1 Oϵ2
		Leu 18 OT2	
W8		Glu 1 N	Glu 1 Oϵ1
		Lys 17 O	
W9		Leu 18 OT1	

[a] The maximum distance allowed between non-hydrogen atoms for consideration as hydrogen bonded is 3.1 Å. OT1 and OT2 refer to the carboxy-terminal oxygens; N and O refer to the amide nitrogen and carboxyl oxygen, respectively.

Two of the nine identified solvent molecules lie within hydrogen bonding distance of only a single neighboring atom: water 1 apparently makes a hydrogen bond only to water 2, and water 9 ligands only to the carboxy terminal oxygen OT2. Because the net charge at neutral pH for this peptide is -1, and there are no solvent channels within the crystal, it is possible that one of the solvent molecules might actually be a sodium ion, yielding a neutral charge within the crystal. This possibility is being investigated by counter-ion replacement experiments with potassium.

The core of the polar interface is dominated by a network of salt bridges that links side chains of antiparallel helices to each other (Fig. 4). No such interactions occur between parallel helices in this interface except at the helix termini (see the Discussion). Three intrahelical salt bridges are observed: Lys 5-Glu 8, Lys 12-Glu 13, and Lys 12-Glu 16. In each pair, the basic residue is closer to the amino terminus with respect to its acidic counterpart. Marqusee and Baldwin (1987) have predicted that single, noninteracting helices should show a different, potentially more stable pattern of intramolecular ion pairing: the acidic residue would be toward the amino terminus with respect to its basic counterpart (e.g., Glu 1-Lys 5, Glu 8-Lys 12, and Glu 13-Lys 17 in peptide F). With this pattern, the dipoles of the salt bridges might have more favorable interactions with the helix dipole (Marqusee & Baldwin, 1987). Because the predicted pattern is not observed, the extensive side-chain interactions between antiparallel helices across the polar interface must minimize the effect of potentially unfavorable dipole interactions. Certainly, the antiparallel association of helices, and hence, the antiparallel alignment of helical macrodipoles, would result in at least partial cancellation of destabilizing intramolecular interactions arising from association with the helix macrodipole.

Phe 9 is the only hydrophobic residue located in the polar interface and is positioned at the helix midpoint. Because of its location, the phenyl ring of Phe 9 makes Van der Waals contacts with the phenylalanine residues from the antiparallel neighbors. The plane of each ring is tilted roughly 45° with respect to the neighboring ring, resulting in a narrow, zig-zagging line of hydrophobic interactions that bisects the hydrophilic interface. Aside from the $\epsilon 1$ oxygen of Glu 13, a largely hydrophobic environment surrounds the phenylalanines via the atoms from other residues in contact with the phenyl rings (e.g., the methylene groups from Lys 12 and Glu 13).

Helix capping via "end-to-end" helix interactions

In many protein structures, the helix termini are stabilized by capping (Presta & Rose, 1988; Richardson & Richardson, 1988; Serrano & Fersht, 1989), which is typically achieved by hydrogen bond formation between an unbonded amide nitrogen at the amino terminus or carboxyl oxygen at the carboxy terminus to the side chain of a neighboring residue on the helix. Intramolecular capping is not seen in this structure; instead, extensive intermolecular capping occurs (Fig. 5). Amide nitrogens of residues 1–3 and two of the three carbonyl oxygens at the carboxy terminus are not involved in helical hydrogen bonds, but are capped via interactions with other helices and solvent molecules.

The network of capping hydrogen bonds between helix termini involves four separate helices, where the helical interactions are along the b-axis (i.e., between parallel helices) or along the

c-axis (i.e., helices abutting end-to-end). In the first case, the parallel capping interactions are mediated by side-chain to main-chain hydrogen bonds (Oϵ of Gln 2 to the neighboring amino terminus and Nζ of Lys 17 to both the carbonyl oxygen of Leu 16 and the carboxy terminal oxygen OT2 on the adjacent helix) as seen in Figure 2A. In the second case, the main-chain atoms are involved in a pattern of hydrogen bonding where one carboxy terminus of one helix ligands to two neighboring amino termini (Fig. 5). The backbone carbonyl oxygen of Lys 17 forms a hydrogen bond with the amino-terminal nitrogen of one end-to-end neighbor and a second hydrogen bond links OT1 of the carboxy terminus and N of Gln 2 of another adjacent end-to-end helix. Conversely, the amino terminus of one helix also makes equivalent interactions with the carboxy termini of two neighbors related by a *c*-axis translation. The net result of capping between neighboring amino and carboxy termini is a continuation of helical hydrogen bonding along the *c*-axis, as observed in the crystal structures of several naturally occurring helical peptides (Karle & Balaram, 1990; Karle et al., 1990).

Discussion

Analysis of the crystal structure reported here highlights three key structural features. First, the tight, parallel packing of amphiphilic helices results in the formation of a flat, continuous rows of helices that generate alternating hydrophobic and hydrophilic interfaces. This feature may be the consequence of the nearly "balanced" ratio of apolar to polar amino acids in peptide F. Second, in the hydrophilic interface, where the helix packing neutralizes the helix macrodipole, water-mediated hydrogen bonds and side-chain interactions from antiparallel-related helices play dominant roles in helix association. Third, adjacent helices form extensive and complementary associations between the termini, most likely arising from the free amino- and carboxy-terminal charges. The presence of these free charges does not interfere with crystallization; in fact, it may actually predispose peptide F toward more extensive intermolecular contacts between the termini.

Aspects of these structural features have been observed in crystal structures of less polar peptides. For example, it has been observed that polar helices pack in an antiparallel arrangement in the crystal (Karle, 1994). Hydrophobic residues have been shown to pack closely together with regular ridges-into-grooves geometry (Karle et al., 1990), although without forming the flat, regular interfaces seen in the Type I crystal structure of peptide F. The segregation of polar and apolar faces of helices has also been observed, as in [Leu^1]zervamicin (Karle et al., 1991). However, peptides such as zervamicin, alamethacin, and melittin are much less polar than Peptide F and thus result in a very limited polar region with few hydrogen bonds or salt-bridge interactions between helices. Only the recent crystal structure of the dodecapeptide α1 (Prive et al., 1995) has revealed a helix-packing arrangement similar to that seen with peptide F (see below). Finally, the transition from α-helical conformation to 3_{10} conformation has also been described in helical peptide structures, but only with peptides containing α-aminoisobutyric acid (Aib) residues, which are strong helix-forming residues and which greatly influence the formation of 3_{10}-helical conformations (Karle & Balaram, 1990). In short, the Type I peptide F structure reveals an interesting combination of several common themes observed in peptide crystal structures and represents an extension of these themes to more polar, non-Aib-containing peptides that are more likely to be observed in globular proteins.

In considering the oligomeric state of peptide F in the crystallization conditions, the observed packing of helices in the Type I crystal form cannot derive directly from the association of discrete six-helix bundles, the state observed in aqueous solution at low salt concentrations (Chin et al., 1992). Moreover, the Type II crystal form, grown in aqueous solution at high salt concentrations (2.5–2.8 M ammonium sulfate), has lattice constants and crystal symmetry that also preclude packing arrangements that are either similar to the Type I crystal packing or that are derived from a six-helix bundle. Peptide F thus exhibits a broad range of discrete, solvent-dependent aggregation states and the structural characteristics that may favor hexamer formation in aqueous solution may also favor other modes of interaction in the presence of organic solvents or high salt.

The packing arrangement of helices in the Type I crystal form is of some interest with regard to the action of magainins (Bechinger et al., 1991; Cruciani et al., 1992; Matsuzaki et al., 1995; Tytler et al., 1995). Magainins and magainin analogues have a considerable degree of surface active properties, although they may only transiently integrate into bilayers as transmembrane helical bundles (Matsuzaki et al., 1995). Type I crystal form demonstrates how an amphiphilic peptide could assemble into an oligomeric species that creates a considerable hydrophobic surface area. The assembly of such large "carpets" of peptides on the surface of a membrane could initiate bilayer deformation that may result in peptide insertion or bilayer discontinuities.

Another peptide system also displays a multitude of discrete, solvent-dependent aggregation states. Hill et al. (1990) described the aggregation behavior of the dodecapeptide α1 in aqueous solution and in the crystalline state. Recently, the structure of a second crystal form of peptide α1 has been determined (Prive et al., 1995). This new crystal form has a distinctly different helix-packing arrangement than in the tetragonal crystal form (Hill et al., 1990), but shows a similar packing arrangement to peptide F Type I crystals: hydrogen bonds between the carboxy terminus of one helix to the amino terminus of a neighboring helix are observed, and rows of aligned helices alternate between regions of hydrophobic and hydrophilic contacts.

The variability of helix packing observed in aggregates of peptides F and α1 highlights how amphiphilicity and a helical conformation may predispose a peptide toward aggregation. An understanding of the ability of solvent and ionic environments to induce helix aggregation into different and unique states could provide insight into how a changing local environment affects biological processes such as protein folding or the integration of protein into biological membranes. It is clear that peptides with a balanced amphiphilic character can be designed to exhibit solubility, helicity, and discrete states of self-assembly over a wide range of polar and apolar solvent conditions. Such amphiphilic peptides might then provide a tool to explore how subtle modifications in the amphiphilicity and solvent environment can alter helix aggregation and to guide for the further design of well-defined, self-aggregating systems.

Materials and methods

Peptide F (EQLLKALEFLLKELLEKL) was synthesized according to Chin et al. (1992). Type I crystals were grown by the

hanging drop vapor diffusion method using 0.2 M Na/K_2PO_4, pH 7.2, and 25% 2-propanol. The monoclinic ($P2_1$) Type I crystals diffract to 1.2 Å. Type II crystals were grown, also by the hanging drop vapor diffusion method, at pH 7.4 in 70% saturated $(NH_4)_2SO_4$ and 5% 2-propanol; the resulting crystals are tetragonal ($P4_22_12$) and diffract to 2.0 Å.

The raw data from Type I crystals, collected with Cu K_α radiation (Elliott GX-21 with a 300-μm focus cup and graphite monochromator and operated at 2.8 kW), were measured to 1.41 Å using a FAST area detector (Enraf-Nonius); data were processed with MADNES (Messerschmidt & Pflugrath, 1987) and PROCOR (Kabsch, 1988), and scaled using the CCP4 package (Collaborative Computational Project, 1994). The merged data (see Table 2) included Mo data from 8.0 to 1.9 Å, scaled with Cu data from 3.0 to 1.5 Å. High-resolution cutoff for the Cu data set was determined by the resolution at which $\langle I \rangle / \langle \sigma I \rangle < 5$. For the Type II crystal form, data were collected with Cu K_α radiation (Elliott GX-21 with a 300-μm focus cup and graphite monochromator, and operated at 2.8 kW) and processed to 2.1 Å in a similar manner as the Type I data.

Two idealized α-helices (an octadeca(alanine) α-helix and an ideal peptide F helix) were constructed and were used as search models for two series of rotation searches using the program XPLOR v. 3.1 (Brünger, 1992), and employing the parameters from Engh and Huber (1991). All rotation solutions in common between the two searches were ranked and then examined with the translation function. The search protocol yielded the proper helix orientation and position within the top 10 rotation/translation function consensus solutions. The poly(alanine) coordinates, corresponding to the top translation function solution, were subjected to rigid-body refinement and simulated-annealing. An iterative model-building/simulated-annealing protocol beginning from a poly(alanine) α-helix allowed the entire structure to be built. Proper orientation along the helical axis could be determined by the presence of density for all side-chain atoms of residues Glu 8 and Phe 9 in the electron density maps phased with a properly oriented and positioned poly(alanine) helix. The final refinement protocol used 2,360 reflections, between 8 and 1.5 Å and with intensities greater than 2 σ, and 162 non-hydrogen atoms (153 peptide and 9 solvent) atoms. The final RMS deviations from ideal geometry were 0.014 Å for bond lengths, 1.4° for bond angles, and 17.0° for torsion angles. The atomic coordinates have been submitted to the Brookhaven Protein Data Bank (entry 1PEF) with a 1-year hold on their release.

Acknowledgments

The work presented here was supported in part by grants from the Human Frontiers Program (R.M.G.), the NIGMS 44158 (N.C.Y), and the University of Chicago. K.S.T. was supported by a PHS/NIH Molecular Biophysics Training Grant. We thank Prof. Robert Scheidt for allowing the use of the small molecule X-ray facility at the University of Notre Dame for data collection. We also thank Dr. Patrick Loll for critical reading of this manuscript.

References

Banerjee U, Tsui F, Balasubramanian T, Marshall G, Chan S. 1983. Structure of alamethicin in solution. One- and two-dimensional 1H nuclear magnetic resonance studies at 500 MHz. *J Mol Biol 165*:757–775.

Bechinger B, Kim Y, Chirlian L, Gesell J, Neumann J, Montal M, Tomich J, Zasloff M, Opella SJ. 1991. Orientations of amphipathic helical peptides in membrane bilayers determined by solid-state NMR spectroscopy. *J Biomol NMR 1*:167–173.

Blundell T, Barlow D, Borkakoti N, Thornton J. 1983. Solvent-induced distortions and the curvature of α-helices. *Nature 306*:281–283.

Brünger A. 1992. *X-PLOR manual, version 3.1*. New Haven, Connecticut: Yale University Press.

Chakrabarti P, Bernard M, Rees D. 1986. Peptide-bond distortions and the curvature of α-helices. *Biopolymers 25*:1087–1093.

Chin T, Berndt K, Yang N. 1992. Self-assembling hexameric helical bundle forming peptides. *J Am Chem Soc 114*:2279–2280.

Choma C, Lear J, Nelson M, Dutton P. 1994. Design of a heme-binding four-helix bundle. *J Am Chem Soc 116*:856–865.

Chothia C, Levitt M, Richardson D. 1981. Helix to helix packing in proteins. *J Mol Biol 145*:215–250.

Collaborative Computational Project, N4. 1994. The CCP4 suite: Programs for protein crystallography. *Acta Crystallogr D 50*:760–763.

Crick F. 1952. Is α-keratin a coiled coil? *Nature 170*:882–883.

Cruciani R, Barker J, Durell S, Raghunathan G, Guy H, Zasloff M, Stanley E. 1992. Magainin 2, a natural antibiotic from frog skin, forms ion channels in lipid bilayer membranes. *Eur J Pharmacol 226*:287–296.

Cruciani R, Barker J, Zasloff M, Chen H, Colamonici O. 1991. Antibiotic magainins exert cytolytic activity against transformed cell lines through channel formation. *Proc Natl Acad Sci USA 88*:3792–3796.

DeGrado W. 1988. Design of peptides and proteins. *Adv Prot Chem 39*:51–124.

DeGrado W, Regan L, Ho S. 1987. The design of a four-helix bundle protein. *Cold Spring Harbor Symp Quant Biol 52*:521–526.

DeGrado W, Wasserman Z, Lear J. 1989. Protein design, a minimalist approach. *Science 243*:622–628.

Engh R, Huber R. 1991. Accurate bond and angle parameters for X-ray protein structure refinement. *Acta Crystallogr A 47*:392–400.

Fox R, Richards F. 1982. A voltage-gated ion channel model inferred from the crystal structure of alamethacin at 1.5-Å resolution. *Nature 300*:325–330.

Handel T, DeGrado W. 1990. De novo design of a Zn^{+2}-binding protein. *J Am Chem Soc 112*:6710–6711.

Handel T, Williams S, DeGrado W. 1993. Metal ion-dependent modulation of the dynamics of a designed protein. *Science 261*:879–885.

Harbury P, Kim P, Alber T. 1994. Crystal structure of an isoleucine-zipper trimer. *Nature 371*:80–83.

Harbury P, Zhang T, Kim P, Alber T. 1993. A switch between two-, three-, and four-stranded coiled coils in GCN4 leucine zipper mutants. *Science 262*:1401–1407.

Hecht M, Richardson J, Richardson D, Ogden R. 1990. De novo design, expression, and characterization of Felix: A four-helix bundle protein of native-like sequence. *Science 249*:884–891.

Hill C, Anderson D, Wesson L, DeGrado W, Eisenberg D. 1990. Crystal structure of α_1: Implications for protein design. *Science 249*:543–546.

Ho S, DeGrado W. 1987. Design of a 4-helix bundle protein: Synthesis of peptides which self-associate into a helical protein. *J Am Chem Soc 109*:6751–6758.

Hu Y, Chin T, Fleming G, Yang N. 1993. Fluorescence study of hexameric helical peptide systems. *J Phys Chem 97*:13330–13334.

Juretic D, Hendler R, Kamp F, Caughey W, Zasloff M, Westerhoff H. 1994. Magainin oligomers reversibly dissipate delta microH+ in cytochrome oxidase liposomes. *Biochemistry 33*:4562–4570.

Kabsch W. 1988. Evaluation of single-crystal X-ray diffraction data from a position sensitive detector. *J Appl Crystallogr 21*:916–924.

Kamtekar S, Schiffer J, Xiong H, Babik J, Hecht M. 1993. Protein design by binary patterning of polar and nonpolar amino acids. *Science 262*: 1680–1685.

Karle I. 1994. Diffraction studies of model and natural peptides. In: S. White, ed. *Membrane protein structure*. New York: Oxford University Press. pp 355–381.

Karle I, Balaram P. 1990. Structural characteristics of α-helical peptide molecules containing Aib residues. *Biochemistry 29*:6747–6756.

Karle I, Flippen-Anderson J, Agarwalla S, Balaram P. 1991. Crystal structure of [Leu^1]zervamicin, a membrane ion-channel peptide: Implications for gating mechanisms. *Proc Natl Acad Sci USA 88*:5307–5311.

Karle I, Flippen-Anderson J, Uma K, Balaram P. 1990. Synthetic peptide helices in crystals: Structure and antiparallel and skewed packing motifs for α-helices in two isomeric decapeptides. *Biopolymers 30*:719–731.

Lear J, Wasserman Z, DeGrado W. 1988. Synthetic amphiphilic peptide models for protein ion channels. *Science 240*:1177–1181.

Lovejoy B, Choe S, Cascio D, McRorie D, DeGrado W, Eisenberg D. 1993. Crystal structure of a synthetic triple-stranded α-helical bundle. *Science 259*:1288–1293.

Lutgring R, Chmielewski J. 1994. General strategy for covalently stabilizing helical bundles: A novel five-helix bundle protein. *J Am Chem Soc 116*:6451–6452.

Marqusee S, Baldwin R. 1987. Helix stabilization by $Glu^{-}\cdots Lys^{+}$ salt bridges in short peptides of de novo design. *Proc Natl Acad Sci USA 84*:8898–8902.

Matsuzaki K, Murase O, Fujii N, Miyajima K. 1995. Translocation of a channel-forming antimicrobial peptide, magainin 2, across lipid bilayers by forming a pore. *Biochemistry 34*:6521–6526.

McLachlan A, Stewart M. 1975. Topomyosin coiled-coil interactions: Evidence for an unstaggered structure. *J Mol Biol 98*:293–304.

Messerschmidt A, Pflugrath J. 1987. Crystal orientation and X-ray pattern prediction routines for area-detector diffractometer systems in macromolecular crystallography. *J Appl Crystallogr 20*:306–315.

Montal M. 1995. Molecular mimicry in channel protein structure. *Curr Opin Struct Biol 5*:501–506.

Oblatt-Montal M, Bühler L, Iwamoto T, Tomich J, Montal M. 1993. Synthetic peptides and four-helix bundle proteins as model systems for the pore-forming structure of channel proteins. *J Biol Chem 268*:14601–14607.

O'Shea E, Klemm J, Kim P, Alber T. 1991. X-ray structure of the GCN4 leucine zipper, a two-stranded, parallel coiled coil. *Science 254*:539–544.

Presnell S, Cohen F. 1989. Topological distribution of four-α-helix bundles. *Proc Natl Acad Sci USA 86*:6592–6596.

Presta L, Rose G. 1988. Helix signals in proteins. *Science 240*:1632–1641.

Prive G, Ogihara N, Wesson L, Cascio D, Eisenberg D. 1995. A designer peptide at high resolution: Shake and bake solution of a 400 atom structure. Montreal, Canada: *Am Crystallogr Assoc Annual Meeting*. pp 149 [Abstr].

Ramachandran G, Sasisekharan V. 1968. Conformations of polypeptides and proteins. *Adv Prot Chem 23*:283–438.

Regan L, Clarke N. 1990. A tetrahedral zinc(II)-binding site introduced into a designed protein. *Biochemistry 29*:10878–10883.

Richardson J, Richardson D. 1988. Amino acid preferences for specific locations at the ends of α helices. *Science 240*:1649–1652.

Robertson D, Farid R, Moser C, Urbauer J, Mulholland S, Pidikiti R, Lear J, Wand A, DeGrado W, Dutton P. 1994. Design and synthesis of multiheam proteins. *Nature 368*:425–432.

Schafmeister C, Miercke L, Stroud R. 1993. Structure at 2.5 Å of a designed peptide that maintains solubility of membrane proteins. *Science 262*:734–738.

Serrano L, Fersht A. 1989. Capping and α-helix stability. *Nature 342*:296–299.

Terwilliger T, Weissman L, Eisenberg D. 1982. The structure of melittin in the form I crystals and its implication for melittin's lytic surface activities. *Biophys J 37*:353–361.

Tytler E, Anantharamaiah G, Walker D, Mishra V, Palgunachari M, Segrest J. 1995. Molecular basis for prokaryotic specificity of magainin-induced lysis. *Biochemistry 34*:4393–4401.

Weber P, Salemme F. 1980. Structural and functional diversity in 4-α-helical proteins. *Nature 287*:82–84.